ATTITUDE DETERMINATION FOR JAPAN'S FIRST INTERPLANETARY FLIGHTS, 'SAKIGAKE' AND 'SUISEI'

K Ninomiya

Institute of Space and Astronautical Science (ISAS)
Tokyo, Japan

N Muranaka & M Uo

NEC Corporation
Space Development Division
Yokohama, Japan

ABSTRACT

The attitude determination system for Japan's Halley explorers "SAKIGAKE" and "SUISEI" consists of a sun sensor(SAS) and a star scanner(STS) and ground based attitude determination software(ADS). The essential feature of ADS is the autonomous star identification (SID) and attitude/bias estimation (ABE). The SID identifies the stars without a priori attitude knowledge utilizing angular separation match technique. The ABE utilizes sequential least-squares method to achieve overall attitude determination accuracy of less than 0.1 degrees. In this paper, the outline of attitude determination system, SID and ABE algorithms, the system verification method, and the flight results are described.

Keywords: Attitude Determination, Star Identification, Bias Estimation, System Verification, Interplanetary Flight, Star Scanner, Sun Sensor

1. INTRODUCTION

"SAKIGAKE" and "SUISEI", Japan's first interplanetary mission for the scientific exploration of Halley's comet, were successfully launched respectively in January and August 1985. The system design of both spacecraft is identical except for their scientific instruments. "SAKIGAKE" carries three scientific instruments : plasma wave probe (PWP), solar wind experiment (SOW), and interplanetary magnetic field experiment (IMF), while "SUISEI" carries energy spectrometer (ESP) and ultra violet imaging camera (UVI). (Ref.1,2)

The requirements placed on the attitude determination system were:

1. overall attitude determination accuracy of less than ±0.1 degrees for UVI.
2. near real-time attitude determination for spacecraft operation and control.
3. attitude determination for arbitrary attitude to cope with variety of delta-V possibility.

To meet these requirements, while taking into account the severe weight restriction, the sensor system aboard the spacecraft was defined to comprise a sun aspect sensor(SAS) and a star scanner (STS), a minimal requisite for attitude determination. Attitude Determination Software (ADS) was prepared on the ground computer to determine spacecraft attitude from the telemetered sensor data.

The system worked effectively and brought the mission to full success. This paper describes the system configuration, algorithm, verification method and flight results of the attitude determination system.

2. ATTITUDE DETERMINATION SYSTEM

2.1 Attitude sensing system

"SAKIGAKE" and "SUISEI" are spin stabilized spacecraft with mechanically despun high gain anten-

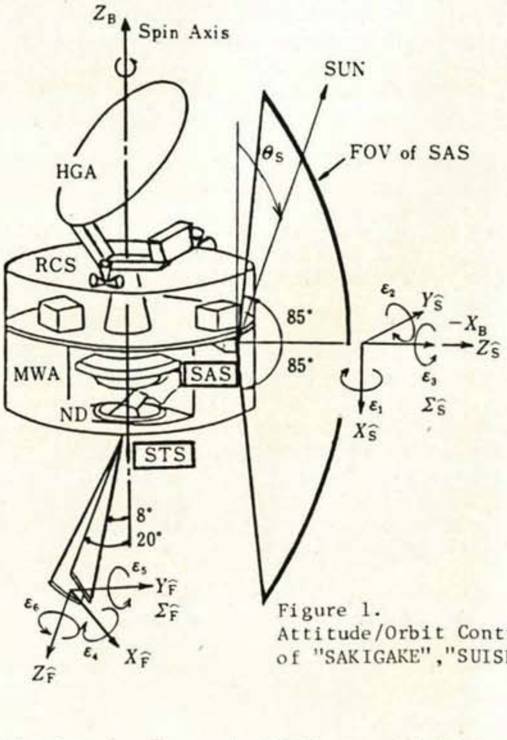

Figure 1.
Attitude/Orbit Control System of "SAKIGAKE","SUISEI"

na (HGA) mounted on the top. The spin rate is about 6.3 rpm in the cruising mode. When UVI takes pictures of the comet, the spin rate is controlled to 0.2 rpm with momentum wheel (MWA). Reaction control system comprised with six 3N thrusters is used for orbit and attitude maneuver.

The attitude sensing system is composed of a spin-type sun sensor (SAS) and a star scanner (STS), developed by ADCOLE Corporation and Ball Aerospace Systems Division respectively (Ref.3,4). Fig.1 shows the configuration of attitude and orbit control system(AOCS).(Ref.5)

The SAS consists of two sensor heads plus two corresponding electronics completely independent functionally. Each sensor head has a thin fan beam shaped field of view (FOV) of 128° and tilt-mounted to each other by 42°. In this way two sensor heads cover FOV of ±85° with respect to the equatorial plane of spacecraft coordinate. The ±43° central portion of FOV is covered by both sensors.

The STS is a passive scan type with two stripe-shaped silicon photodiodes placed on the focal plane of the optical system forming a "V"-like shape. The sensor optical axis is tilted at an angle of 14 degrees from minus Z axis of the spacecraft so as to use Canopus (α-Carinae) as main target star for attitude determination. Two photodiode elements subtend fan beam shaped FOV of 12° ,one FOV is nominally parallel to spin axis and the other inclined about 20° with respect to the first. The outputs of the photodiodes are merged together to provide a common star signal output. Fig.2 shows the typical shape of star signal. STS holds the peak of the signal and outputs star coincidence pulse when the star signal falls below the half of the peak level.

The sensor data is processed in attitude and orbit control electronics(AOCE) and telemetered to the ground station in the form of sun angle(θ_S), interval between the sun pulses (spin period), interval between the sun pulse and star pulses, and star intensity.

2.2 Software system

Telemetry data received by 64m ϕ antenna at USUDA Deep Space Center (UDSC) is transferred to KOMABA Deep Space Operation Center (KDSC) through dedicated communication lines. The data is stored in the central computer in which AOCS support software system resides. The software system includes ADS, AOCS command generation software, and orbit determination software.

ADS consists of three sub-softwares:

(1) Real-time ADS (ADS-RT)
This software determines and displays the attitude in real time.

(2) Delay-time ADS (ADS-DT)
This software is used for precise analysis of the attitude history after the fact.

(3) Bias estimation software (ADS-BIAS)
This software is dedicated to the estimation of biases such as sensor misalignments and tilt angles. Only the telemetry obtained while the spacecraft is static (nutation ≈ 0) is picked up for the estimation and the result is fed back to ADS-RT and ADS-DT.

The basic algorithm used in these sub-softwares are essentially the same. The software flow was adapted to each software purpose.

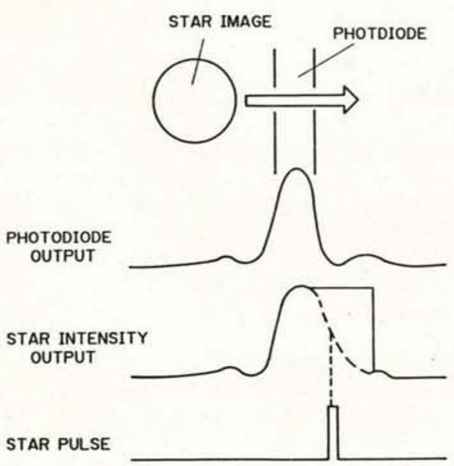

Figure 2. STS Star Pulse Output

3. ATTITUDE DETERMINATION ALGORITHM

Two major aspects of the attitude determination algorithm lie in star identification (SID) and attitude and bias estimation (ABE).

As the SAS and STS are the only attitude sensors onboard the spacecraft, no prior attitude knowledge is expected for star identification. An angular separation match technique was employed to find candidate attitude for which phase match technique was applied to select final attitude or to confirm the selected attitude.(Ref.6) In this way SID provides initial (coarse) attitude, and the attitude is refined by ABE utilizing sequential least-squares method. In ADS-BIAS, biases such as sensor misalignments are also estimated along with the attitude.

The procedure of SID and ABE will be briefly described below.

3.1 Coordinate system

The software is implemented based on the coordinate systems described below.

Σ_I : Inertial coordinate
Sun centered ecliptic of 1950.

Σ_B : Body coordinate
Body fixed frame in which Z axis is along intended spin axis and -X axis in nominal SAS mounting plane.

Σ_M : Spin axis coordinate
This frame is obtained by rotation of θ_X and θ_Y from Σ_B (Fig.3) so that Z axis coincideswith the spacecraft true spin axis. The true spin axis coincides with the spacecraft principal axis of inertia while the momentum wheel is off. θ_X and θ_Y then represent spacecraft dynamic imbalance. While the wheel is rotating, the true spin axis coincides with wheel rotation axis, for the wheel holds almost all the

angular momentum of the spacecraft. Then, θ_X and θ_Y are recognized as wheel misalignments.

$\Sigma_S, \Sigma_F, \Sigma_{\tilde{S}}, \Sigma_{\tilde{F}}$:

Σ_S and Σ_F denote the true SAS and STS frame respectively. The superscript ~ denotes the nominal frame. The true frame is obtained by small angle rotation that represents the sensor misalignments. The misalignments include mounting error and deviation caused by launch shock and/or thermal distortion.

$\Sigma_{\tilde{S}}$, $\Sigma_{\tilde{F}}$ and Σ_B are depicted in Fig.1. Transformation matrices between these coordinate systems are written as follows.

$$T_{M.B}=\begin{pmatrix} 1 & 0 & -\theta_X \\ 0 & 1 & -\theta_Y \\ \theta_X & \theta_Y & 1 \end{pmatrix}$$

$$T_{\tilde{S}.B}=\begin{pmatrix} 0 & 0 & -1 \\ 0 & -1 & 0 \\ -1 & 0 & 0 \end{pmatrix}, \quad T_{\tilde{F}.B}=\begin{pmatrix} 0 & u & -v \\ -1 & 0 & 0 \\ 0 & v & u \end{pmatrix}$$

$$u=\cos 166^\circ \quad v=\sin 166^\circ$$

$$T_{S.\tilde{S}}=\begin{pmatrix} 1 & \varepsilon_3 & -\varepsilon_2 \\ -\varepsilon_3 & 1 & \varepsilon_1 \\ \varepsilon_2 & -\varepsilon_1 & 1 \end{pmatrix}, \quad T_{F.\tilde{F}}=\begin{pmatrix} 1 & \varepsilon_6 & -\varepsilon_5 \\ -\varepsilon_6 & 1 & \varepsilon_4 \\ \varepsilon_5 & -\varepsilon_4 & 1 \end{pmatrix}$$

where $T_{Y.X}$ denotes the transformation from Σ_X to Σ_Y.

3.2 Star identification (SID)

3.2.1 Pulse averaging The SID starts collecting star pulses for five spacecraft spin period to obtain 'clean' star data. Pulses that appear at the same phase and with the same intensity are grouped together. Groups with more than three pulses are judged to be effective. Pulse data is averaged in the group and the result is used as basic pulse data for star identification.

3.2.2 Pulse pairing As the star scanner outputs two star pulses for a star, it is necessary to find out the pulse pair produced by the same star. The basic conditions to be satisfied to form a pair are:

a. Intensity of the pulses are the same within a predetermined error
b. Phase separation between the pulses are larger than the minimum separation of two photodiodes and smaller than the maximum separation of the diodes

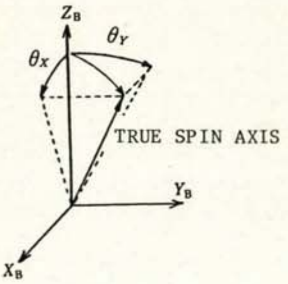

Figure 3.
Definition of θ_X and θ_Y

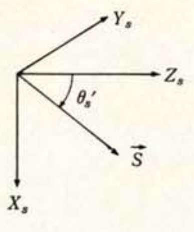

Figure 4.
Definition of θ_s'

The pair is considered to be 'reliable' if:

c. each pulse of the pair forms a pair only with the partner.

At first, the software searches reliable pairs. If no reliable pairs are found, a pair that satisfies conditions a. and b. only is searched.

SID process is carried out for the pairs thus presumed. If the SID fails, a new pair is selected and SID is executed again.

3.2.3 Separation matching The separation matching procedure is divided into two phases: sun-star matching and star-star matching.

Using the direction vector computed for the presumed pair, separation angle between the sun and the presumed star, expressed in Σ_B, is computed as the reference angle. Catalog stars whose position is separated by the reference angle from the sun and whose magnitude is similar to that of the presumed star are extracted from star catalog. If plural reliable pairs exist, angular separations between the pairs are compared with the separations of catalog stars. Thus, candidates for matching are extracted. If no candidates remain, the pairing is assumed to be at fault and the pairing process takes place again.

The star catalog contains about 300 stars brighter than the 3rd magnitude and planets such as Venus and Mars. Magnitude of the stars are compensated for according to the spectrum of the stars.

3.2.4 Coarse attitude determination

For further extraction of candidates in the case where plural catalog stars remain as candidates for a pair, and also for confirmation of the case in which only one catalog star is matched with a pair, a coarse attitude is computed for each candidate and then star pulse pattern that would be obtained for the attitude is simulated to be compared with the data pulse pattern (phase match technique).

In simulating star pulse patterns, the following STS peculiarities were taken into account.

(1) In the condition that two (or more) consecutive pulses occur in a short period, the latter pulse does not appear affected by the former (Fig.5(a)). This is called as 'dead time' effect.
(2) The star signal has three peaks as shown in Fig.2. This can result,in case of bright stars, in STS's detecting the first peak as a star position. The true star signal does not appear because of the 'dead-time' effect. (Fig.5(b)) This is called as 'three peaks effect'.

In principle, these irregularity should be avoided by controlling the sensor threshold level.

For coarse attitude determination, the so called matrix method often used for 3-axis attitude determination is utilized; Let $\vec{s}$ and $\vec{\lambda}$ denote the sun and star vector expressed in Σ_{M0} which is Σ_M at the instance of SAS sun crossing. Let $\vec{S}$ and $\vec{\Lambda}$ denote the sun and star vector in Σ_I. Then the spin axis vector $\vec{a}$ is computed as follows.

$$\vec{a}=T_{M_0I}\begin{pmatrix}0\\0\\1\end{pmatrix}\qquad T_{M_0I}=M(\vec{S},\vec{\Lambda})M^T(\vec{s},\vec{\lambda})\tag{1}$$

$$M(\vec{x},\vec{y})\triangleq\begin{pmatrix}\vec{x}^T\\(\vec{x}\times\vec{y})^T/|\vec{x}\times\vec{y}|\\(\vec{x}\times(\vec{x}\times\vec{y}))^T/|\vec{x}\times\vec{y}|\end{pmatrix}^T$$

3.2.5 Star tracking Once the pulses are identified, they are compared with the data pulses obtained successively. Only the pulses that match with the identified pulses are used in ABE. If the matching fails for more than five consecutive trials, the SID is initialized again. This process allows us to execute burdensome star identification process only at the initialization phase.

3.3 Attitude and bias estimation (ABE)

As the nutation of the spacecraft is quickly damped by nutation damper, the ABE is designed on the basis that the spacecraft nutation is negligibly small. Before the nutation is damped, only the coarse attitude is determined.

Parameters included in this algorithm are spacecraft attitude, tilt angles, and sensor misalignments. In ADS-RT and ADS-DT, only the attitude is estimated. Biases are estimated only in ADS-BIAS.

The basic observation equations are:

$$\begin{pmatrix}\sin\theta'_s\\0\\\cos\theta'_s\end{pmatrix}=T_{S.\tilde{S}}T_{\tilde{S}.B}T_{B.M}T_{M.M_0}T_{M_0I}\vec{S}\tag{2}$$

$$\vec{a}_i\cdot(T_{F.\tilde{F}}T_{\tilde{F}.B}T_{B.M}\Omega(\omega_s t)T_{M.M_0}T_{M_0I}\vec{\Lambda})=0\tag{3}$$

$\vec{a}_i$ denotes normal vector of STS FOV plane expressed in Σ_F (i=1,2). $T_{M.M_0}$ is the error matrix of the true attitude from the attitude obtained by eq.(1). $\Omega(\theta)$ denotes the rotation of θ about Z axis. ω_s and t denotes the spin rate and star pulse timing respectively. The definition of θ'_s is depicted in Fig.4.

The former equation is for SAS data and the latter is based on the fact that the slit normal vector is orthogonal to the star vector when the star pulse occurs.

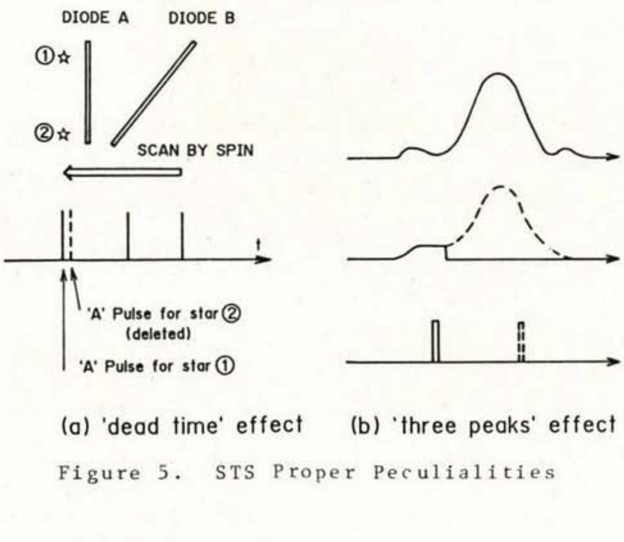

Figure 5. STS Proper Peculialities

As the error of coarse attitude can be assumed to be small, $T_{M.M_0}$ is written as

$$T_{M.M_0}=\begin{pmatrix}1&\psi&-\theta\\-\psi&1&\varphi\\\theta&-\varphi&1\end{pmatrix}\tag{4}$$

and eq.(2) and (3) can finally be rearranged to the following form.

$$\sin\theta'_s=-S'_X(\theta-\varepsilon'_2)-S'_Z\tag{5}$$

$$(\vec{a}\cdot\vec{\varphi})\varphi+(\vec{a}\cdot\vec{\theta})\theta+(\vec{a}\cdot\vec{p})\varepsilon^*_4+(\vec{a}\cdot\vec{q})\varepsilon'_5+(\vec{a}\cdot\vec{r})\varepsilon^*_6+(\vec{a}\cdot\vec{c})=0\tag{6}$$

where

$$\vec{\varphi}=\begin{pmatrix}uc\Lambda'_Z+v\Lambda'_Y\\-s\Lambda'_Z\\vc\Lambda'_Z-u\Lambda'_Y\end{pmatrix}+\frac{S'_Z}{S'_X}(u\vec{r}-v\vec{p})\qquad\vec{\theta}=\begin{pmatrix}us\Lambda'_Z-v\Lambda'_X\\c\Lambda'_Z\\vs\Lambda'_Z+u\Lambda'_X\end{pmatrix}$$

$$\vec{p}=\begin{pmatrix}0\\(c\Lambda'_Y-s\Lambda'_X)v+u\Lambda'_Z\\c\Lambda'_X+s\Lambda'_Y\end{pmatrix},\quad\vec{q}=\begin{pmatrix}(s\Lambda'_X-c\Lambda'_Y)v-u\Lambda'_Z\\c\Lambda'_Z\\vs\Lambda'_Z+u\Lambda'_X\end{pmatrix}$$

$$\vec{r}=\begin{pmatrix}-(c\Lambda'_X+s\Lambda'_Y)\\(s\Lambda'_X-c\Lambda'_Y)u+v\Lambda'_Z\\0\end{pmatrix}$$

$$\vec{c}=\begin{pmatrix}(c\Lambda'_Y-s\Lambda'_X)u-v\Lambda'_Z\\-(c\Lambda'_X+s\Lambda'_Y)\\(c\Lambda'_Y-s\Lambda'_X)v+u\Lambda'_Z\end{pmatrix}+\frac{S'_Y}{S'_X}(u\vec{r}-v\vec{p})$$

$$c=\cos\omega_s t,\quad s=\sin\omega_s t$$

$$(\Lambda'_X\ \Lambda'_Y\ \Lambda'_Z)^T=\vec{\Lambda}'\triangleq T_{M_0I}\vec{\Lambda}$$

$$(S'_X\ S'_Y\ S'_Z)^T=\vec{S}'\triangleq T_{M_0I}\vec{S}$$

$$\varepsilon^*_4=\varepsilon'_4-v(\varepsilon'_1-\frac{S'_Z}{S'_X}\varepsilon'_3)\tag{7}$$

$$\varepsilon^*_6=\varepsilon'_6+u(\varepsilon'_1-\frac{S'_Z}{S'_X}\varepsilon'_3)\tag{8}$$

$$\begin{array}{ll}\varepsilon'_1=\varepsilon_1 & \varepsilon'_4=\varepsilon_4-u\theta_X\\\varepsilon'_2=\varepsilon_2+\theta_X & \varepsilon'_5=\varepsilon_5-\theta_Y\\\varepsilon'_3=\varepsilon_3-\theta_Y & \varepsilon'_6=\varepsilon_6-v\theta_X\end{array}\tag{9}$$

These equations imply that unknown parameters φ, θ, ψ, ε_1, ε_2, ε_3, ε_4, ε_5, ε_6, θ_X, and θ_Y can not be independently estimated but only be estimated in the form: φ, θ, ε'_2, ε^*_4, ε'_5, and ε^*_6. More than 3 stars must be observed to estimate all these six parameters. Sequential least-squares method was applied to estimate these parameters. Estimated ε'_2, ε^*_4, ε'_5, and ε^*_6 are used in ADS-RT and ADS-DT.

Spin axis $\vec{a}$ is obtained by the following equation with the estimated φ and θ.

$$\vec{a}=(\sin\theta,\ -\sin\varphi\cos\theta,\ \cos\varphi\cos\theta)T_{M_0I}\tag{10}$$

4. VERIFICATION OF ADS

To verify the performance of ADS, SDGS (Sensor Data Generation Software) was developed to simulate sensor outputs that will be obtained in orbit. In SDGS, the mathematical model of SAS, STS, orbit and attitude dynamics, and spacecraft telemetry processing functions are constructed and used to generate the outputs.

As the proper processing of STS data was considered as the key to ADS success, STS was carefully modeled so that the simulated output would realize the actual STS operation faithfully. This was based on the tests using a star simulator and also field test. Fig.6 shows the STS model adopted in SDGS. Input to point (a) is modeled from the actual output of the light detectors for star simulator or actual star light. Furthermore, background signal created by Galactic light and Zodiacal light is calculated and are added. Fig.7 shows an example of simulated star input signal to point (a). This example shows the case in which the spacecraft spin axis is perpendicular to the ecliptic plane.

ADS verification by SDGS was performed in two ways. One is to generate telemetry file whose format is identical with the actual one. ADS can read and process the file directly. This test was performed principally to verify attitude determination accuracy.

The other is to stimulate the actual sensors with simulated sensor inputs. The purposes of this test are:

1. to verify that ADS properly processes actual sensor data
2. to check the total data transmission system and to verify the compliance of ADS with the system

SDGS outputs the sensor input signals as numerical data train onto magnetic tape. The tape is brought to spacecraft test facility and mini-computer converts the data to analog signals with its D/A converter and stimulates the sensors through interface circuitry.

STS is stimulated by LED (Light Emitting Diode) set up on the hood cover which protects STS from dust on the ground. The current of the LED is controlled so that the brightness may vary as shown in Fig.7. Sun signals are configured so that they will be identical with the sensor head outputs and are inputted to the SAS electronics.

In this manner, telemetry data that reflects actual sensor characteristics and actual spacecraft telemetry processing functions is obtained. The telemetry data is stored into telemetry processing computer and fed to ADS. In parallel, telemetry stream signal is recorded into analog tape recorder. The tape recorder is brought to UDSC and the data is inputted to the telemetry processor. The telemetry data is transferred to KDSC through data communication links in the same manner as the actual operation. ADS was operated in real time and was verified that it would work in the actual operation.

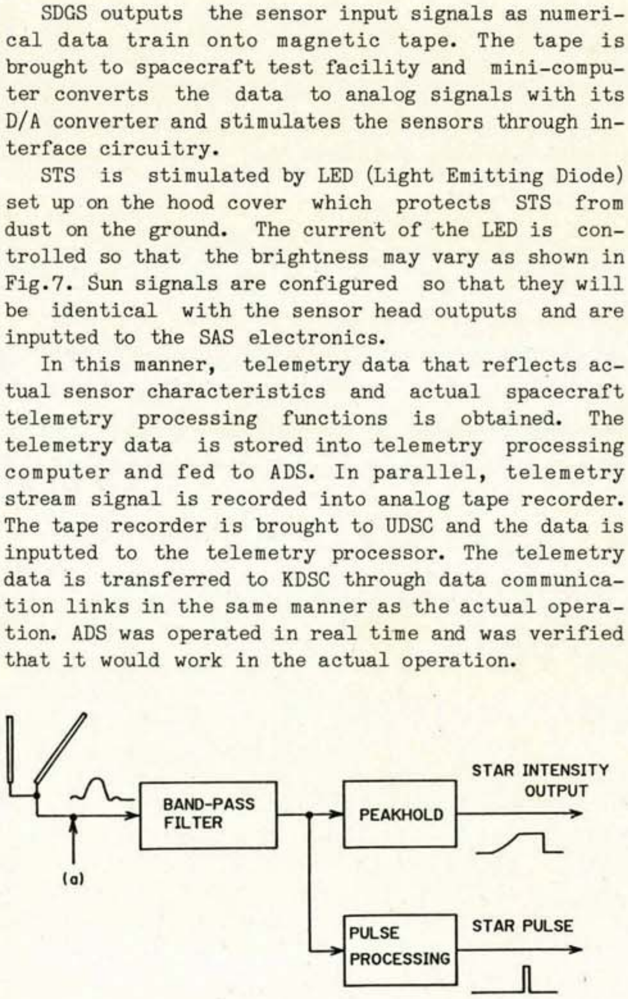

Figure 6. STS Model in SDGS

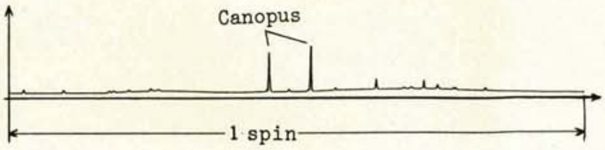

Figure 7. Simulated STS input

5. FLIGHT RESULTS

The spacecraft were brought into cruising attitude after two days from the launch by M-3S-II vehicle and encountered Halley's comet in March 1986. The performance of attitude determination system during these period is discussed below.

5.1 Sensor performance

Jitter of Sun angle and Sun detection timing of SAS as well as the jitter of STS star pulses for Canopus were all less than 0.01° which were slightly better than the value expected during the prelaunch evaluation. Canopus was detected as a star of about -0.98 mag while the expected magnitude was -0.89 mag. For dark stars, it was difficult to determine the actual magnitude for the effect of background light. The maximum error was about 0.9 mag. The darkest star that STS detected was that of about 2.5 mag for which detection was very sensitive to the background. Fig.8 is an example of star data. 'Three peaks' effect mentioned in section 3 is shown in the figure.

In the case of "SAKIGAKE" spurious pulses whose intensity exceed the saturation level of STS output were seen on the ground with the count rate of about 2 pulses/hour. In orbit, the rate increased to 4 - 9 pulses/hour on the average and about 70 pulses/hour at the maximum. These pulses are considered to be induced by cosmic rays, especially by solar cosmic ray flux because the period the rate increased almost corresponds to the period when the solar flare emerged. In case of "SUISEI" the rate of spurious response was less than that of "SAKIGAKE". This might have been due to the difference of photodiode characteristics such as thickness of silicon layer.

5.2 Star Identification

When the STS was first turned on in the initial operation phase, it observed the Southern Cross ("SAKIGAKE") and stars of the Eridanus ("SUISEI"). After several attitude maneuvers including that for orbit correction, the spacecraft were brought into cruising attitude (spin axis perpendicular to the ecliptic plane) and STS acquired Canopus and the neighboring stars. These stars were successfully identified except in the case:

(1) spurious pulses appeared so frequently that they were not filtered out by pulse averaging process before the spacecraft nutation was damped.
(2) pulses of Canopus vanished for the 'three peaks' effect, and no other effective stars were in the FOV of STS.

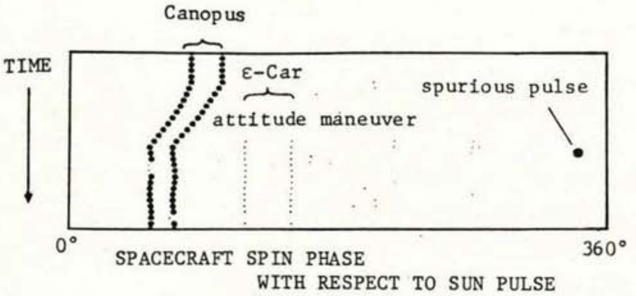

The dots represent the star pulses.
The size of the dots expresses the intensity of the pulses.

Figure 8. Example of STS Star Pulse Data

5.3 Bias estimation

As was expected, the random noise of SAS and STS was very small. Therefore biases are considered large compared with the random noise, thus dominating the attitude determination error.

In the cruising attitude, STS observed Canopus, ε-Car, β-Car, and sometimes R-Dor (variable star). This enabled us to estimate all the parameters shown in eq.(5-6). The estimation results are evaluated as follows.

ε_2 and ε_5 are the alignment parameters most accurately measured on the ground among the others. Assuming these were not changed during the launch, the tilt θ_X and θ_Y were estimated by

$$\theta_X = \varepsilon_2' - \varepsilon_2 \quad (11)$$

$$\theta_Y = \varepsilon_5 - \varepsilon_5' \quad (12)$$

Let $\bar{\varepsilon}^*_1$ and $\bar{\varepsilon}^*_6$ denote the calculated value using thus determined θ_X and θ_Y and ε_1, ε_3, ε_4, ε_6 value measured on the ground. $\Delta\varepsilon^*_1$ and $\Delta\varepsilon^*_6$, the differences between $\bar{\varepsilon}^*_1$, $\bar{\varepsilon}^*_6$ and estimated ε^*_1, ε^*_6 will indicate the fitness between the estimation and the actual.

Table 1. shows the obtained θ_X, θ_Y, $\Delta\varepsilon^*_1$ and $\Delta\varepsilon^*_6$ and their accuracy. The estimation accuracy of θ_X, θ_Y is, according to eq.(11) and (12), calculated as route sum square of estimation accuracy of ε_2', ε_5' and measurement accuracy of ε_2, ε_5. The value in the brackets are measurement accuracy of θ_X, θ_Y on the ground. The table shows the estimation error of less than 0.1 degrees. (The large error in $\Delta\varepsilon^*_6$ is caused by ε_6 measurement error for which precise measurement was impossible.)

The estimation error is considered to be caused by:

(1) error of FOV normal vector $\vec{\alpha}$ in Σ_F caused by measurement error and unmodeled bias sources such as STS focal length and optical distortion
(2) shift of star pulses by background light

6. CONCLUSION

The configuration, algorithm, verification method, and flight results of the attitude determination system for Japan's Halley explorers "SAKIGAKE" and "SUISEI" were described.

The system worked satisfactory; stars were automatically identified, and the expected attitude determination accuracy was attained through estimation of biases such as tilts and misalignments.

7. ACKNOWLEDGMENT

The authors wish to express the appreciation to those who participated in the project, especially to Mr. Masahiro Ogasawara, Miss Hoshiko Aoki, and Mr. Masafumi Kimura for their significant contribution to the software development.

8. REFERENCES

1. T.Nomura, T.Hayashi & H.Hirosawa et al.1981, Deep Space Projects in Japan, AIAA/NASA Symposium on SpaceTracking and Data Systems, June, 1981
2. K.Hirao & H.Matsuo 1982, Japanese Halley Exploration Project, IAF-82-191
3. ADCOLE Corporation, Feb. 1981, Equipment Specification Spin Type Fine Sun Sensor for Satellite Use (SFSS)
4. R.L.Gutshall & G.Z.Thomas 1979, Pioneer Venus Star Sensor, AAS 79-004
5. K.Ninomiya & K.Uesugi et al. 1984, PLANET-A Atti-Attitude and Orbit Control System, AAS 84-006
6. J.R.Wertz et al. 1978, Spacecraft Attitude Determination and Control, D.Reidel Publishing Company

Table 1. Bias Estimation Result

SPACECRAFT	SAKIGAKE		SUISEI	
WHEEL	OFF	ON	OFF	ON
HGA DESPUN	ON	OFF	ON	OFF
θ_X	-0.012±0.024 (*)	-0.020±0.037 (0.007±0.023)	0.030±0.027 (*)	0.072±0.018 (0.050±0.023)
θ_Y	-0.042±0.047 (*)	-0.057±0.023 (0.017±0.023)	0.081±0.048 (*)	0.016±0.017 (0.023±0.023)
$\Delta\varepsilon^*_1$	0.007±0.004 (0±0.052)		0.087±0.004 (0±0.052)	
$\Delta\varepsilon^*_6$	0.171±0.060 (0±0.201)		0.187±0.049 (0±0.201)	

* $\sqrt{\theta_X^2 + \theta_Y^2} \leq 0.06°$